Geochemistry and sedimentary environments

SHRIMP zircon U−Pb ages from coal beds across the Permian−Triassic boundary, eastern Yunnan, southwestern China

Juan Wang [a,b], *Long-Yi Shao* [a,*], *Hao Wang* [a], *Baruch Spiro* [c], *David Large* [d]

[a] *State Key Laboratory of Coal Resources and Safety Mining, College of Geoscience and Surveying Engineering, China University of Mining and Technology (Beijing), Beijing 100083, China*
[b] *School of Resources and Environment, Henan Polytechnic University, Jiaozuo 454003, Henan Province, China*
[c] *Department of Mineralogy, The Natural History Museum, London SW7 5BD, United Kingdom*
[d] *Faculty of Engineering, University of Nottingham, Nottingham NG7 2RD, United Kingdom*

Abstract   The first SHRIMP zircon U−Pb ages from coal beds close to the end-Permian mass extinction are reported from the C_1 coal seam in the Yantang Mine in Laibin Town, Xuanwei County, eastern Yunnan Province. Zircons were extracted from kaolinite claystone layers, defined as tonsteins (volcanic ash deposits), in the sub-seam B_1 and B_3 of the coal seam C_1. The U−Pb ages are 252.0 ± 2.3 Ma and 250.3 ± 2.1 Ma for the sub-seam B_1 and B_3, respectively. Within analytical uncertainties, these U−Pb ages include the time period of the onset of the mass extinction at 251.941 ± 0.037 Ma, which was obtained from the marine Meishan section in Zhejiang Province, ~1600 km away from the Yantang Mine. These new ages represent not only the first and closest ages to the PTB mass extinction in terrestrial coal beds, but also ages from the nearest site to the Emeishan volcanoes investigated so far. Therefore these new data provide the most accurate stratigraphic horizon of terrestrial facies of the end-Permian extinction in South China. The Emeishan volcanoes were likely the source of volcanic ash in the coal seams at the Xuanwei County and broader areas in South China. Furthermore, the minerals and geochemistry characteristics of the C_1 coal seam also implied the influences of contemporaneous volcanic activities.

Keywords   PTB mass extinction, C_1 coal seam, SHRIMP U−Pb isotope age, Xuanwei County, Yunnan Province

1.   Introduction

End-Permian time is one of the most important critical transitions in Earth's history, and the largest mass extinction occurred at the Permian—Triassic transition. According to detailed studies mainly in the Meishan Global Stratotype Section and Point (GSSP) section, Zhejiang Province, southeastern China, the main mass extinction pulse happened just before the defined Permian—Triassic boundary (PTB) (Shen *et al.*, 2011; Yin and Song, 2013; Yin *et al.*, 2001, 2012), the main episode of the end-Permian mass extinction and PTB age were constrained as 251.941 ± 0.037 Ma and 251.902 ± 0.024 Ma (Burgess *et al.*, 2014), respectively. The peak mass extinction occurred just before 252.28 ± 0.08 Ma at Meishan section, and lasted no more than 200 ± 100 thousand years (kyr) (Shen *et al.*, 2011; Yin *et al.*, 2012). The PTB age obtained from different sections varies to some degree due to the precision of dating methods and possibly-incomplete stratigraphic record in some sections. So far, most of the PTB ages are from clay beds (bentonite) in marine sections, and few reliable PTB ages from terrestrial sections, particularly from the Permian coal beds that are widespread in South China.

The eastern Yunnan Province of southwestern China has well-preserved terrestrial Permian strata including coal beds that may cross the time of the PTB. Coal-bearing strata in eastern Yunnan belong to the Upper Member of the Upper Permian Xuanwei Formation. The uppermost Xuanwei Formation contains the C_1 coal seam which is overlain by the Kayitou Formation of the Lower Triassic. Because coal beds may record important information about the palaeoclimate and palaeoecological changes across the PTB in terrestrial environments, the age of the C_1 coal seam would be a critical anchor for establishing the time-framework of events surrounding the end-Permian mass extinction.

In this paper, we report the first U—Pb SHRIMP ages of the C_1 coal seam in the Yantang Mine in Xuanwei County, eastern Yunnan Province. Zircons are collected from the tonsteins in the C_1 coal seam, which have formed from contemporaneous volcanic eruptions according to the mineralogical and geochemical evidences. With the new age data, we discuss the end-Permian mass extinction and PTB in coal-bearing terrestrial sections, as well as their correlation with the marine records (Shen *et al.*, 2011; Yin and Song, 2013; Yin *et al.*, 2012).

2.   Geological setting

During the Late Permian, the study area, Xuanwei County, eastern Yunnan Province, was located in the western Yangtze Craton of the South China Block (Fig. 1; Wang and Jin, 2000). Siliciclastic sediments in this area were supplied predominantly from the Khangdian Oldland (Fig. 1B) in the west. Controlled by transgression from the east throughout the Late
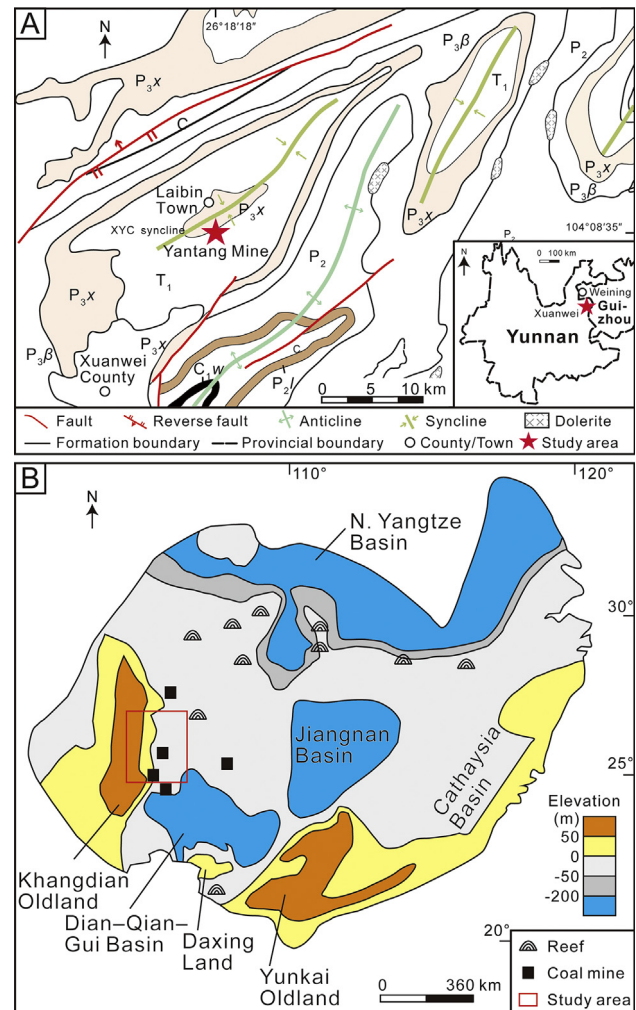
Fig. 1 A — Simplified geological map of the Xuanwei County, eastern Yunnan Province, southeastern China (modified from Shao *et al.*, 2015). C = Carboniferous; C_1w = Wanshoushan Formation of the Carboniferous; P_2 = Middle Permian; P_2l = Liangshan Formation of the Middle Permian; $P_3\beta$ = Emeishan Basalt Formation of the Upper Permian; P_3x = Xuanwei Formation of the Upper Permian; T_1 = Lower Triassic; XYC syncline = Xiangyangcun syncline; B — Palaeotectonic features of the South China (modified from Wang and Jin, 2000).

Permian, and the sedimentary environments in eastern Yunnan and western Guizhou during Late Permian vary from marine, transitional to terrestrial facies from east to west. The Xuanwei Formation of Late Permian in Xuanwei County is mainly terrestrial fluvial facies (Shao *et al.*, 1998; Wang *et al.*, 2011). The C_1 coal seam comprises low—medium volatile bituminous coal with a low to medium-high ash yield and a very low sulfur content (Shao *et al.*, 2015).

The sedimentary sequence surrounding the Permian—Triassic boundary (PTB) in the eastern Yunnan Province consists of a series of intercalated siltstone and mudstone overlain by coal seams of Late Permian age (Peng *et al.*, 2001, 2005; Shao *et al.*, 2012), and thin-medium layers of fine sandstone, siltstone, pelitic siltstone, silty mudstone of earliest Triassic age. The Upper Permian in Xuanwei County comprises the Xuanwei Formation, which unconformably overlies the Emeishan Basalt, and is in turn conformably overlain by the Kayitou Formation of the Lower Triassic (Fig. 2). The Xuanwei Formation, consists mainly of gray fine-grained sandstone, siltstone and mudstone, some volcanic ash beds, and numerous coal seams including the C_1 coal seam at the top (Dai *et al.*, 2008). The Yantang Mine sequence sampled in this study is located near the Xiangyangcun syncline with small faults developed on both sides of the mine area (Fig. 1A).
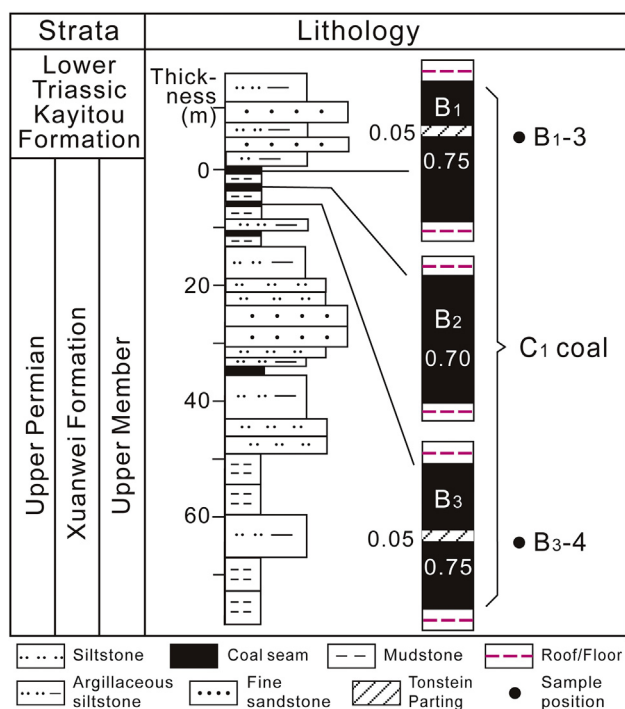

Fig. 2 Stratigraphical and lithological profile of the Yantang Mine, eastern Yunnan Province. The position and thickness of the minable coal seams and tonstein partings are marked.

3. Sampling and analysis

3.1. Sampling

Samples from the C_1 coal seam were collected from the Yantang Mine, located in Laibin Town, northeastern Xuanwei County (Fig. 1A). The C_1 coal seam consists of the B_1, B_2 and B_3 sub-seams in descending order in this mine (Fig. 2). No further coal seams occur above B_1 until the Middle Triassic, marking the onset of the global "coal gap" during the Early Triassic (Retallack *et al.*, 1996; Shao *et al.*, 2000). The three sub-seams (B_1, B_2 and B_3) are the only minable seams in the Yantang Mine, and their thicknesses at the sampling sites are 0.75 m, 0.70 m and 0.75 m, respectively. The spacing between sub-seams B_1 and B_2, B_2 and B_3 are 2.73 m and 3.39 m, respectively. In addition, within the sub-seams B_1 and B_3, there are two layers of volcanic ash (tonstein) (Zhou *et al.*, 2000) with a thickness of about 5 cm each.

The characteristics of the three sub-seams in the Yantang Mine are as follows:

1) The B_1 coal lies at the top of the Xuanwei Formation, with a thickness of 0.75 m. This sub-seam contains a kaolinite claystone parting (tonstein) with a thickness of 5 cm. Its roof and floor are both carbonaceous mudstone.
2) The B_2 coal lies 2.73 m below the B_1 coal. The thickness of the B_2 coal is 0.70 m, and no parting is presented inside. The roof and floor are also carbonaceous mudstone.
3) The B_3 coal lies 3.39 m below the B_2 coal. The thickness of the B_3 coal is 0.75 m, with a 5-cm-thick kaolinite claystone parting (tonstein) inside. The roof of this sub-seam is silty mudstone and the floor is gray mudstone. Evidence for tonstein is discussed in Section 4.1.

Two tonstein samples B_1-3 and B_3-4 were collected from the underground coal face in the Yantang Mine. The coordinates of the sample site are N 26°18′18″ and E 104°08′35″. Each sample collected is ≥2 kg and all the samples were immediately stored in plastic bags to ensure as little contamination as possible.

3.2. Methods

3.2.1. Mineral analysis

The mineralogical composition of the tonstein samples (B_1-3 and B_3-4) was examined by scanning electron microscopy coupled with an energy dispersive

X-ray analyzer (SEM-EDX) and powder X-ray diffraction (XRD). Samples were broken into small pieces first; then the fresh and smooth surfaces of samples were selected and were coated with a very thin layer of gold film. The micro-morphology of minerals was observed and determined by SEM (JSM-6390LV) equipped with EDX (INCA-ENERAGY 250).

Sample B_1-3 was crushed and ground to less than 200 mesh and directly analyzed by powder XRD. Sample B_3-4 was crushed and ground to less than 200 mesh, then further subjected to low-temperature ashing (LTA) in an EMITECH K1050X Plasma Asher. After that, the LTA ashes were analyzed by XRD (Bruker D8 Advance). The XRD patterns were collected in the 2θ range of $5°-90°$ using Cu Kα radiation. The SEM-EDX and XRD analyses of tonstein were carried out at the Key Laboratory of Biogenic Traces and Sedimentary Minerals of Henan Province, Henan Polytechnic University.

3.2.2. Zircon U—Pb dating

The two tonstein samples, each about 1 kg, were crushed and sieved to 60 mesh. The zircon grains were separated using standard heavy liquid from light minerals (such as feldspar and quartz), then using magnetic techniques from magnetic minerals (magnetite, *etc*.). Zircon separation was carried out at the Hebei Institute of Geological Minerals Investigation. Approximately 100 zircon grains were hand-picked from each sample under a binocular microscope, and then mounted on an adhesive tape, enclosed in epoxy resin together with several grains of standard zircon TEMORA. The mount was polished to expose the grain interiors. In order to examine internal textures of zircons, cathodoluminescence (CL) images of individual zircon grains were obtained using Hitachi S-3000N scanning electron microscope (SEM) operating at an accelerating voltage ~10 KV and ion beam current ~10 μA. The zircons were dated in the Sensitive High Resolution Ion Microprobe II (SHRIMP II) at the Beijing SHRIMP Centre, Chinese Academy of Geological Sciences. Detailed analytical procedures and data reduction followed those described by Song *et al.* (2002).

Spots that have the following features are avoided for analysis: textural complexity, rounded grains, and grains containing bubbles, fracture and inclusions. Those zircon grains with uniform CL color, long columnar structure and oscillatory zoning according to CL images were selected for dating (Liu *et al.*, 2011).

Zircons were analyzed for U, Th and Pb using the SHRIMP II. Five scans through the mass stations were carried out for each age determination. The standard zircon was analyzed first and after every three unknown analyses. The TEMORA zircon, with an age of 417 Ma (Black and Jagodzinski, 2003), was used as a standard. The raw ICP-MS data was processed using the ICPMSDataCal procedures, and the ages of zircons were the weighted means calculated using the Isoplot 3.7 programs (Ludwig, 2003), and measured ^{204}Pb was applied for the common lead correction. The uncertainties for individual analysis are quoted at the 1σ confidence level, whereas errors for the weighted mean ages are quoted at the 95% confidence level.

4.   Results

### 4.1.   Mineralogical evidence for tonstein

The mineral composition in the two partings is similar. The XRD results show that kaolinite is the dominant mineral in the partings, followed by quartz, calcite, and minor anatase and ankerite (Fig. 3). Kaolinite occurs in the form of "accordion" and "vermicular" aggregates in B_1-3 and B_3-4, respectively (Fig. 4A and B). No zircons are identified in the partings using SEM-EDX and XRD. However, numerous zircon grains were hand-picked under a binocular microscope from these partings. The CL images (Fig. 4C and D) for zircon grains of the two samples have high length/width ratios and clear oscillatory zoning indicative of volcanic origin (Hoskin and Schaltegger, 2003; Wu and Zheng, 2004). The vermicular texture of kaolinite aggregates are often interpreted as volcanogenic origin (Zhou *et al.*, 2000). In addition, magmatic zircons in volcanogenic tonstein partings are different from the zircons in sediments of terrigenous origin (Zhou and Ren, 1994). Hence, combining the mineral composition and micro-morphological characteristics, the two partings are identified as tonsteins — the products of alteration of volcanic ash.

4.2.   SHRIMP U—Pb age data

U—Pb isotope analyses were conducted on 15 and 16 zircon grains, respectively, for B_1-3 and B_3-4 (Fig. 5). The CL images show that most of the zircon grains are euhedral with elongated prism or blocky shape, $100-400$ μm long. The high length/width ratios and clear oscillatory growth zoning of the zircons indicate their volcanic origin (Hoskin and Schaltegger, 2003; Wu and Zheng, 2004). All the determinations were carried out on the oscillatory zones.

The analytical results are summarized in Table 1 and concordia diagrams are shown in Fig. 6. The Th/
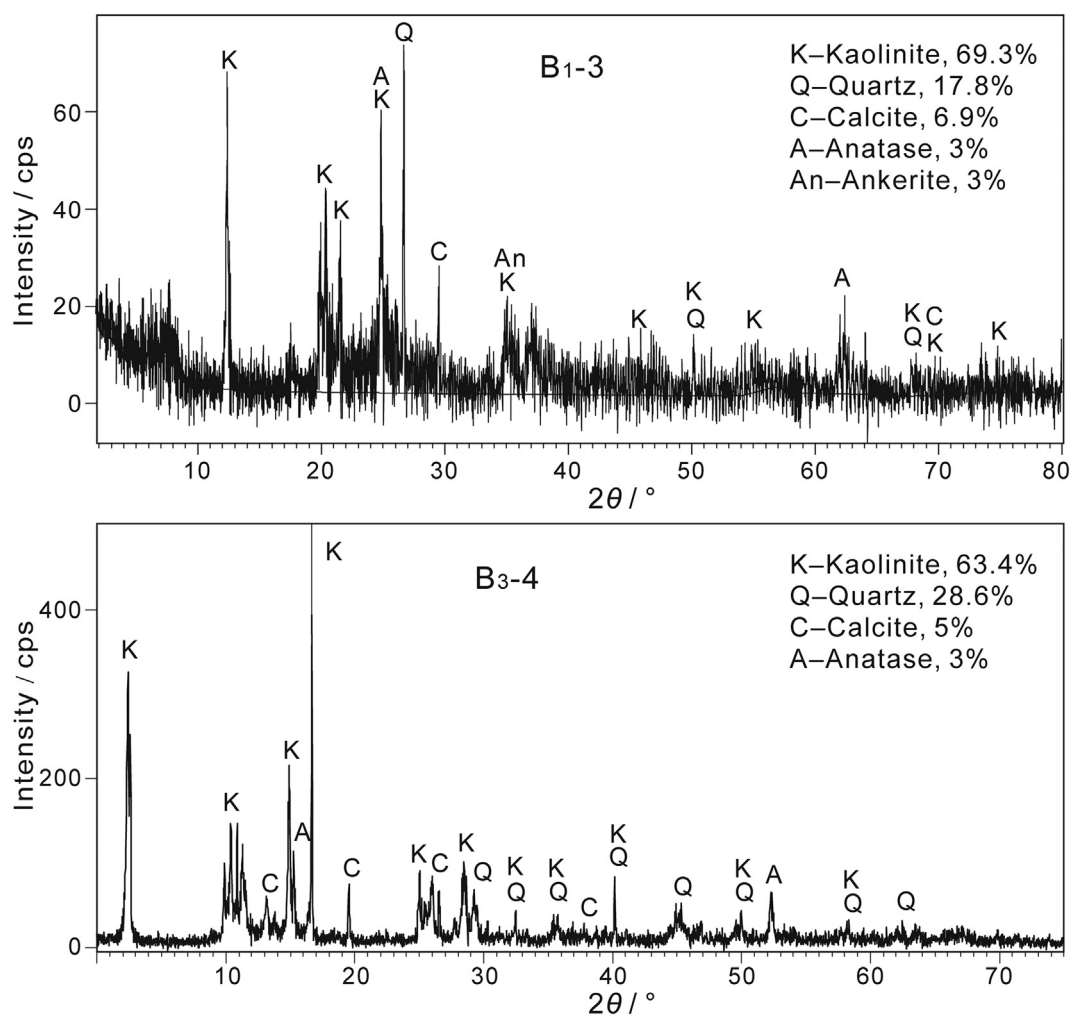
Fig. 3 XRD patterns of the two parting samples B$_1$-3 (powder) and B$_3$-4 (LTA ash) from the Yantang Mine, eastern Yunnan Province. See Fig. 2 for the sampling position.

U ratios of zircons are generally taken as indicators for their conditions of formation. In general, the Th/U ratio of magmatic zircons is greater than 0.4, while that of metamorphic zircons is less than 0.1 (Li *et al.*, 2014). In this study, most of the Th/U ratios of analyzed zircons are greater than 0.4, mostly in the range 0.6–1.2, except for B$_1$-3-7.1 with 0.39. The high Th/U ratios and distinct oscillatory growth zoning observed in CL images (Fig. 5) indicate that all these zircon grains are of igneous origin.

For sample B$_1$-3, the three outliers (spot No. 1.1, 2.1, and 3.1) were discarded because they are significantly abnormal compared with other 12 spots (Table 1). The analyses 1.1 and 3.1 are outliers due to the distinct higher common Pb (^{206}Pb$_c$) content and yielding younger ages than others. The analysis 2.1 is also an outlier because its age is far less than other data. When these three analyses are discarded, the scatter decreases considerably (MSWD = 0.60). The Th

and U concentrations of the other 12 zircons change from 56 ppm to 427 ppm and from 101 ppm to 639 ppm, respectively, with Th/U ratios changing from 0.39 to 0.74. When the age of a sample is younger than 1000 Ma, the ^{206}Pb/^{238}U ages are preferred because they have smaller uncertainties than the ^{207}Pb/^{206}Pb and ^{208}Pb/^{232}Th ages (Black and Jagodzinski, 2003; Compston *et al.*, 1992). Hence, the ^{206}Pb/^{238}U ages are used in present study. The concordia diagrams and the weighted mean calculations were made using the Isoplot 3.7 software (Ludwig, 2003). Excluding the three spots (1.1, 2.1 and 3.1) which have anomalously young ^{206}Pb/^{238}U ages of 247.0 Ma, 240.3 Ma and 234.7 Ma, respectively, the remaining 12 spots yielded ages between 248.1 Ma and 258.8 Ma, with a weighted mean ^{206}Pb/^{238}U age of 252.0 ± 2.3 Ma (n = 12, MSWD = 0.60) (Fig. 6A and C).

For the sample B$_3$-4, there are 12 valid analyses, while the other 4 analyses (spot No. 9.1, 10.1, 13.1 and
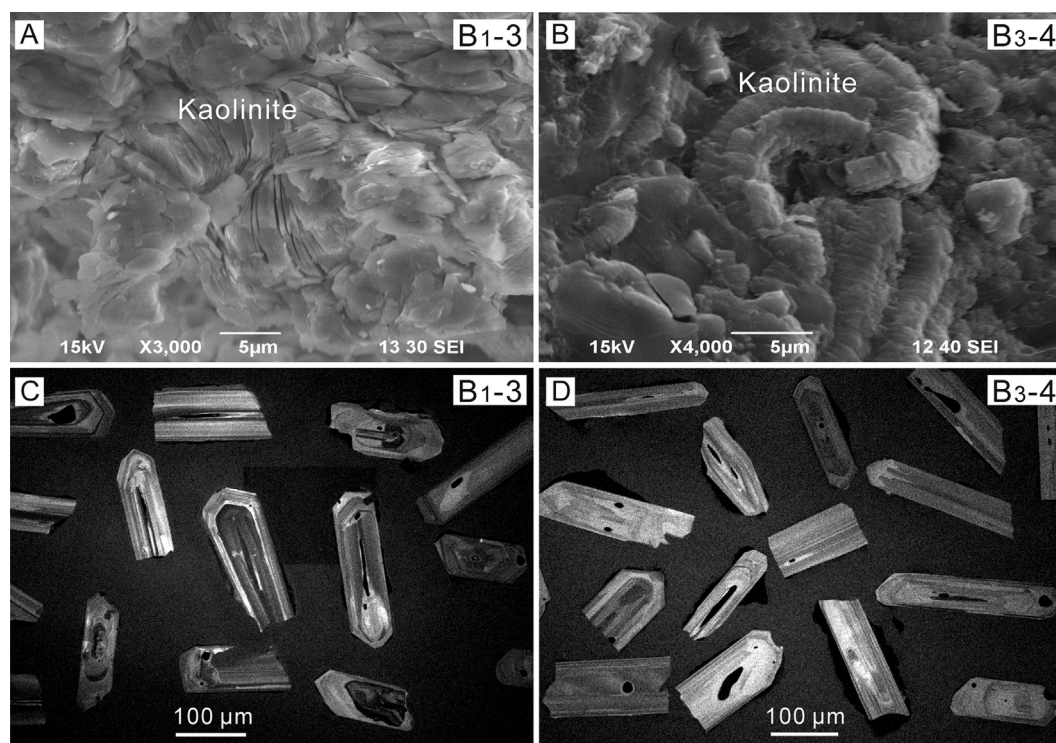
Fig. 4 A and B — SEM images showing the mineral compositions of the two parting samples: accordion kaolinite aggregates in B_1-3 (A); and vermicular kaolinite aggregates in B_3-4 (B); C and D — CL images of the zircons from B_1-3 and B_3-4, showing high length/width ratios and clear oscillatory zoning.

14.1) are obviously discordant (Table 1). The Th and U concentrations of these valid zircons vary from 40 ppm to 516 ppm and from 56 ppm to 346 ppm, respectively. The Th/U ratios range from 0.71 to 1.49. The four abnormal analyses give either too young or too old $^{206}Pb/^{238}U$ ages, which therefore are excluded from the age calculation. The remaining 12 spots yield ages between 244.8 Ma and 259.8 Ma. They are concordant (Fig. 6B and D) and yield a weighted mean $^{206}Pb/^{238}U$ age of 250.3 ± 2.1 Ma (n = 12, MSWD = 1.09).

We interpret the two single-crystal SHRIMP zircon U-Pb ages of samples B_1-3 and B_3-4 represent the formation ages of the tonsteins in the C_1 coal seam. In other words, these ages represent the deposition ages of volcanic ash beds. Furthermore, these ages can be taken as a good approximation for age of the C_1 coal seam because its total thickness is no more than 3 m.

5.   Discussion

5.1.   U−Pb ages of typical PTB sections in South China

The Permian−Triassic timescale has undergone major revisions in recent years based on isotope dilution thermal ionization mass spectrometry (ID-

TIMS) dating of zircons in volcanic ash beds of different locations. Most of these results were obtained from the clay beds adjacent to the PTB sections in South China (Figs. 7 and 8), presently the most accurate PTB age is 251.902 ± 0.024 Ma from Meishan section, Zhejiang Province, southeastern China (Burgess et al., 2014).

Many PTB sections were studied in South China, including sedimentary sequences deposited in marine, terrestrial and transitional environments (Burgess et al., 2014; Gao et al., 2013; Shen et al., 2011; Yang et al., 2005; Yin and Song, 2013; Yin et al., 2007, 2012). Many of these sedimentary sections contain more than one layer of volcanic ash (Bowring et al., 1998), and their dating results can be compared to the ones obtained in this study, as both samples are derived from layer of volcanic ashes (tonsteins), and by the same dating method.

Some previous studies on the radiometric ages of PTB sections in South China are shown in Fig. 8. Of them, the Meishan and Chahe sections are very important, which represent marine and terrestrial sequences, respectively. The Yantang Mine is the geographically close to the Chahe section (68 km) and is also a terrestrial PTB sequence (Fig. 7). The C_1 coal seam of Yantang Mine can be compared to the PTB horizons in Meishan and Chahe sections as all of these
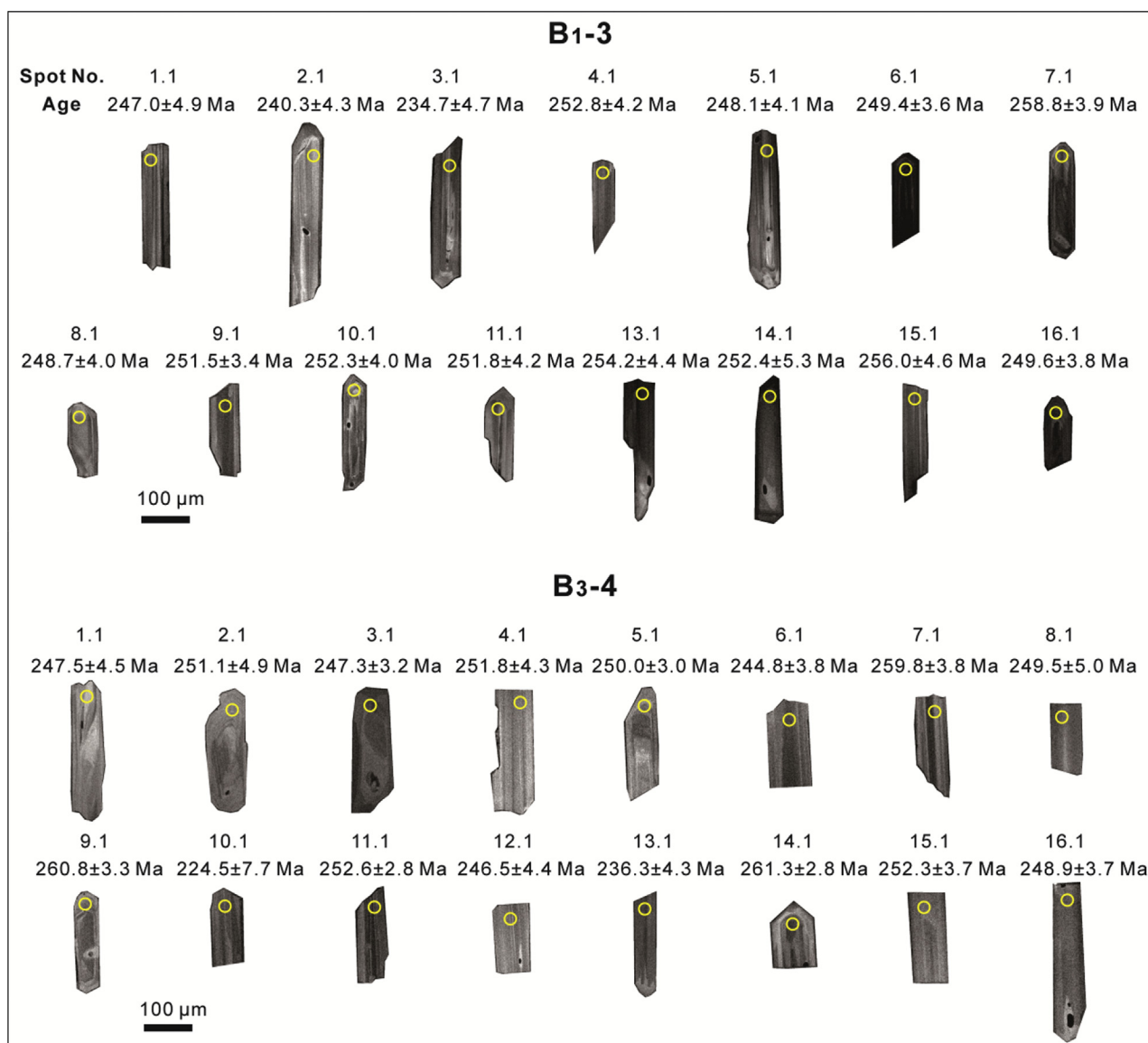
Fig. 5 Representative CL images of zircons from the tonstein partings in coal seams in the Yantang Mine, eastern Yunnan Province. The SHRIMP analytical sites are marked with yellow circles. A total of 31 analyses are shown, 15 from B_1-3 and 16 from B_3-4, respectively.

sections were developed with the similar volcanic ash beds in South China.

The Meishan section located at Meishan town, Changxing County, Zhejiang Province, and described as a well-preserved, continuous marine succession across the Late Permian and Early Triassic, and is the most intensively studied PTB section (Bowring et al., 1998; Burgess et al., 2014; Mundil et al., 2004; Shen et al., 2011; Yin and Song, 2013; Yin et al., 2001, 2012). Here we compare the ages of the Meishan section with those of Yantang Mine, which represent marine and terrestrial deposits, respectively. In the Meishan section it is generally accepted that the PTB lies at the base of Bed 27c, and Beds 25 to 28 are considered as the main extinction beds, essentially Bed 25, which

contains the main episode of the end-Permian mass extinction (Fig. 8; Burgess et al., 2014; Shen et al., 2011; Yin et al., 2014). The latest U—Pb age of Bed 25 is dated as 251.941 ± 0.037 Ma (Burgess et al., 2014). The age of upper sub-seam B_1 from Yantang Mine is 252.0 ± 2.3 Ma, slightly older than 251.941 ± 0.037 Ma. In other words, the time of deposition of the C_1 coal seam of Xuanwei Formation is a little earlier than Bed 25 of the marine Meishan section, which means the coal-forming plant of C_1 coal seam occurred just before end-Permian mass extinction. Maybe the C_1 coal seam, especially the sub-seam B_1, is the witness of the terrestrial end-Permian mass extinction.

Yang et al. (2005) and Yin et al. (2007) suggested that Bed 67 of the Chahe section is equivalent to Bed

Table 1 SHRIMP results and U—Pb ages of zircon grains from the tonstein partings in the Yantang Mine, eastern Yunnan Province.

Spot No.	Content/ppm					Isotope ratio			Isotope age/Ma		
	Th	U	Th/U	^{206}Pb	^{206}Pb$_c$	^{207}Pb/^{206}Pb	^{207}Pb/^{235}U	^{206}Pb/^{238}U	^{208}Pb/^{232}Th	^{207}Pb/^{206}Pb	^{206}Pb/^{238}U
B$_1$-3-1.1	87	133	0.65	4.68	4.40	0.0203 ± 49	0.109 ± 49	0.0391 ± 2.0	145.0 ± 31	−2570 ± 2100	247.0 ± 4.9
B$_1$-3-2.1	104	103	1.01	3.41	1.21	0.0428 ± 12	0.224 ± 12	0.0380 ± 1.8	236.0 ± 11	−176 ± 290	240.3 ± 4.3
B$_1$-3-3.1	143	159	0.90	5.33	4.88	0.0160 ± 55	0.082 ± 55	0.0371 ± 2.0	172.0 ± 19	−3780 ± 3300	234.7 ± 4.7
B$_1$-3-4.1	123	198	0.62	6.87	0.91	0.0442 ± 11	0.244 ± 11	0.0400 ± 1.7	228.0 ± 16	−100 ± 260	252.8 ± 4.2
B$_1$-3-5.1	144	209	0.69	7.17	1.75	0.0384 ± 15	0.208 ± 15	0.0392 ± 1.7	209.0 ± 17	−459 ± 400	248.1 ± 4.1
B$_1$-3-6.1	185	314	0.59	10.70	0.99	0.0546 ± 6.1	0.297 ± 6.3	0.0394 ± 1.5	253.0 ± 11	397 ± 140	249.4 ± 3.6
B$_1$-3-7.1	115	293	0.39	10.30	0.31	0.0496 ± 6.3	0.280 ± 6.5	0.0410 ± 1.5	245.0 ± 16	176 ± 150	258.8 ± 3.9
B$_1$-3-8.1	82	178	0.46	6.08	0.98	0.0457 ± 8.6	0.248 ± 8.8	0.0393 ± 1.6	204.0 ± 17	−19 ± 210	248.7 ± 4.0
B$_1$-3-9.1	427	639	0.67	21.90	0.19	0.0507 ± 2.7	0.278 ± 3	0.0398 ± 1.4	244.0 ± 5.6	227 ± 62	251.5 ± 3.4
B$_1$-3-10.1	131	247	0.53	8.53	0.92	0.0502 ± 11	0.276 ± 11	0.0399 ± 1.6	236.0 ± 21	204 ± 250	252.3 ± 4.0
B$_1$-3-11.1	84	114	0.74	3.95	1.26	0.0423 ± 5.4	0.232 ± 5.7	0.0398 ± 1.7	236.4 ± 8.2	−211 ± 140	251.8 ± 4.2
B$_1$-3-13.1	56	101	0.55	3.54	0.94	0.0495 ± 5.8	0.275 ± 6.1	0.0402 ± 1.7	243.0 ± 11	173 ± 140	254.2 ± 4.4
B$_1$-3-14.1	102	171	0.60	5.95	1.26	0.0534 ± 11	0.294 ± 11	0.0399 ± 2.2	239.0 ± 21	344 ± 250	252.4 ± 5.3
B$_1$-3-15.1	71	108	0.66	3.80	1.20	0.0465 ± 7.2	0.259 ± 7.4	0.0405 ± 1.8	227.0 ± 11	21 ± 170	256.0 ± 4.6
B$_1$-3-16.1	138	252	0.55	8.63	0.84	0.0484 ± 7	0.263 ± 7.2	0.0395 ± 1.5	215.0 ± 13	118 ± 170	249.6 ± 3.8
B$_3$-4-1.1	57	60	0.95	1.59	1.59	0.0413 ± 13	0.223 ± 13	0.0391 ± 1.8	234.0 ± 12	−269 ± 330	247.5 ± 4.5
B$_3$-4-2.1	96	123	0.78	0.43	0.43	0.0475 ± 9.3	0.260 ± 9.5	0.0397 ± 2.0	243.0 ± 13	74 ± 220	251.1 ± 4.9
B$_3$-4-3.1	156	171	0.91	0.76	0.76	0.0461 ± 4.9	0.249 ± 5.1	0.0391 ± 1.3	243.5 ± 6.7	5 ± 120	247.3 ± 3.2
B$_3$-4-4.1	87	86	1.01	1.47	1.47	0.0410 ± 16	0.225 ± 16	0.0398 ± 1.7	224.0 ± 14	−288 ± 410	251.8 ± 4.3
B$_3$-4-5.1	235	219	1.07	0.71	0.71	0.0454 ± 5	0.248 ± 5.1	0.0395 ± 1.2	238.9 ± 5.9	−33 ± 120	250.0 ± 3.0
B$_3$-4-6.1	130	114	1.14	1.40	1.40	0.0409 ± 14	0.218 ± 14	0.0387 ± 1.6	235.0 ± 11	−295 ± 350	244.8 ± 3.8
B$_3$-4-7.1	148	107	1.38	0.89	0.89	0.0451 ± 6.3	0.256 ± 6.5	0.0411 ± 1.5	252.0 ± 7	−48 ± 150	259.8 ± 3.8
B$_3$-4-8.1	40	56	0.71	0.59	0.59	0.0517 ± 8.7	0.281 ± 9	0.0395 ± 2.0	243.0 ± 14	273 ± 200	249.5 ± 5.0
B$_3$-4-9.1	152	172	0.88	0.48	0.48	0.0886 ± 4.2	0.504 ± 4.4	0.0413 ± 1.3	325.9 ± 7.9	1395 ± 81	260.8 ± 3.3
B$_3$-4-10.1	89	93	0.96	1.44	1.44	0.0447 ± 8.4	0.218 ± 9	0.0354 ± 3.5	220.0 ± 11	−73 ± 200	224.5 ± 7.7
B$_3$-4-11.1	516	346	1.49	0.68	0.68	0.0482 ± 5.3	0.265 ± 5.4	0.0400 ± 1.1	240.9 ± 4.6	107 ± 130	252.6 ± 2.8
B$_3$-4-12.1	69	75	0.92	1.68	1.68	0.0427 ± 16	0.229 ± 16	0.0390 ± 1.8	223.0 ± 15	−188 ± 390	246.5 ± 4.4
B$_3$-4-13.1	107	95	1.13	1.21	1.21	0.0483 ± 9.9	0.248 ± 10	0.0373 ± 1.8	227.5 ± 9.8	112 ± 230	236.3 ± 4.3
B$_3$-4-14.1	244	398	0.61	0.30	0.30	0.0514 ± 3.2	0.293 ± 3.3	0.0414 ± 1.1	243.4 ± 6.6	260 ± 73	261.3 ± 2.8
B$_3$-4-15.1	163	140	1.16	0.88	0.88	0.0507 ± 7.4	0.279 ± 7.5	0.0399 ± 1.5	241.5 ± 8.1	228 ± 170	252.3 ± 3.7
B$_3$-4-16.1	109	103	1.06	1.61	1.61	0.0408 ± 9	0.221 ± 9.1	0.0394 ± 1.5	226.5 ± 8.6	−300 ± 230	248.9 ± 3.7

Note: ^{206}Pb$_c$: common Pb; while others are radiogenic Pb.

27 of the Meishan section which is considered as the P/T boundary bed, and the beds from lower 66f to upper 68 (including 68a and 68c) are defined as the boundary interval. The clay beds in 68a and 68c above the PTB at the Chahe section are dated at 247.5 ± 2.8 Ma and 252.6 ± 2.8 Ma, respectively (Yang *et al.*, 2005; Yin *et al.*, 2007). Therefore, the age of Bed 67 should be slightly older than Bed 68a dated as 252.6 ± 2.8 Ma. Shen *et al.* (2011) also gave a similar age of 252.30 ± 0.07 Ma for Bed 68 of the Chahe section. However, they proposed that the age of Bed 68 is comparable with that of Bed 25 at the Meishan section, which is the main extinction bed. Thus, the age of the PTB at the Chahe section should be slightly younger than 252.30 ± 0.07 Ma (Shen *et al.*, 2011). This conclusion seems to be different from the view of Yin *et al.* (2007) and Yang *et al.* (2005), with the differences focusing on whether the PTB is above or below Bed 68.

The marine—terrestrial transitional Zhongzhai section in Liuzhi, Guizhou Province, also contains ash beds across the PTB. The SHRIMP zircon U-Pb ages of the beds immediately above and below the boundary are 252.00 ± 0.08 Ma and 252.24 ± 0.13 Ma, respectively (Shen *et al.*, 2011). Therefore, the age of the PTB at the Zhongzhai section ranges from 252.00 ± 0.08 Ma to 252.24 ± 0.13 Ma.

Gao *et al.* (2013) suggested that the SHRIMP zircon U—Pb ages from the 10 beds across the Permian—Triassic transition of marine Daxiakou section range from ~248.5 Ma to ~253.8 Ma, mostly 250—251 Ma. Lehrmann *et al.* (2015) reported a new U—Pb zircon age of 251.985 ± 0.097 Ma from the PTB at the Taiping section (Guizhou Province), Nanpanjiang Basin in South China.

The International Chronostratigraphic Chart of 2017 showed the latest revised PTB age at 251.902 ± 0.024 Ma, which was reported by International Commission on Stratigraphy (ICS).
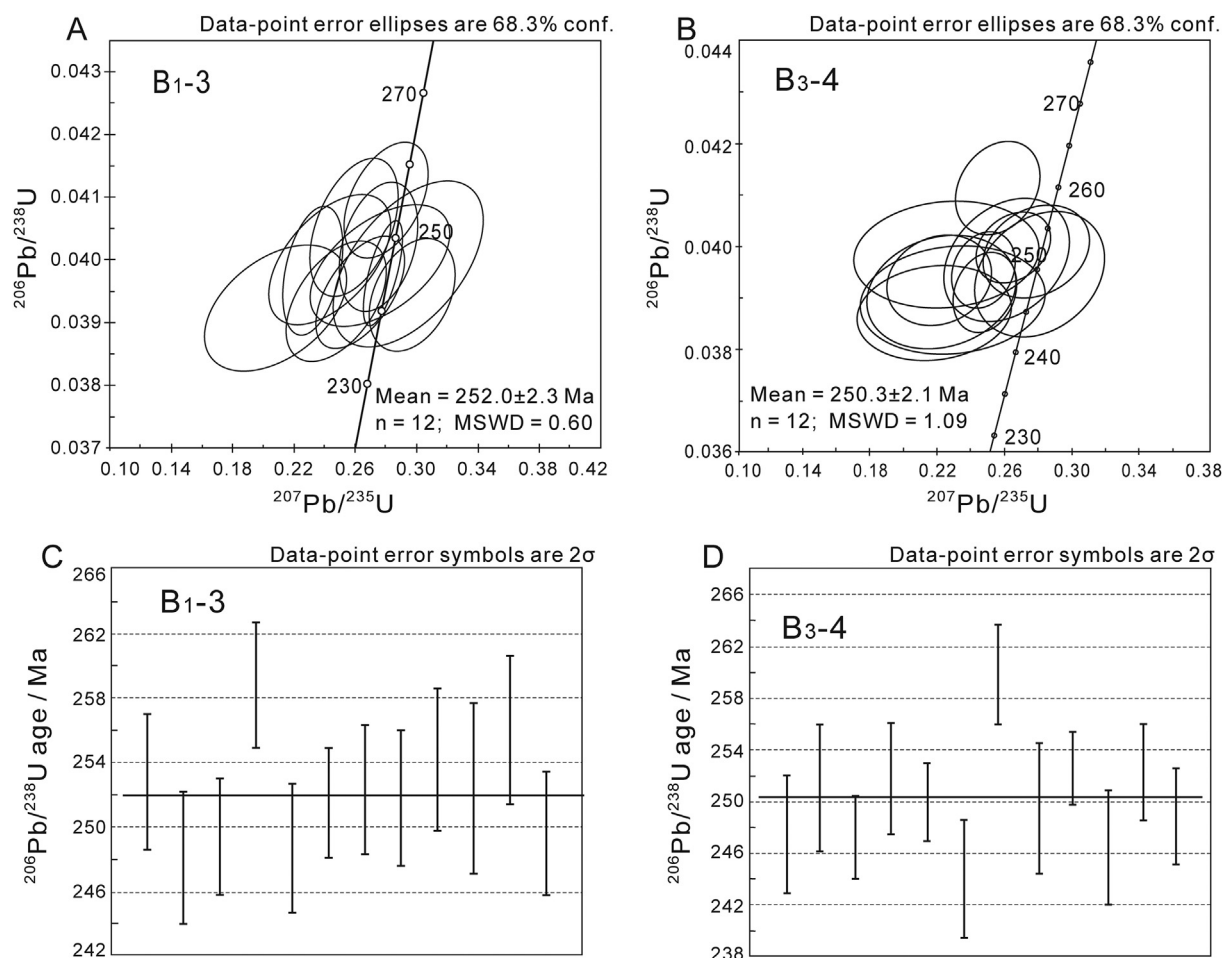
Fig. 6 SHRIMP U–Pb concordia diagrams (A and B) and the age distributions (C and D) of zircon grains from the tonstein-parting samples B_1-3 and B_3-4 in the Yantang Mine. The abnormal values are not shown. See Table 1 for the compilation of analyses.

The $^{206}Pb/^{238}U$ age of the tonstein B_1-3 with 252.0 ± 2.3 Ma is a little older than that of the extinction peak, while much older than those obtained from the PTB at the marine Meishan section in Zhejiang Province, some 1600 km away, where the PTB age determined by ICS (2017) is 251.902 ± 0.024 Ma. Although the age of the B_3-4 is younger than that of the B_1-3, the value ranges of two tonstein layers overlap, indicating that these values are still in a reasonable range. As a whole, the age of C_1 coal seam in the Yantang Mine is very close to the main episode of PTB mass extinction.

5.2. Correlation of the C_1 coal seam and PTB study

Several studies focused on dating the PTB strata by conodont zones (as defined by first appearance datum of the conodont *Hindeodus parvus*) and radiometric ages (Jiang *et al.*, 2007; Kozur, 2003;

Nicoll *et al.*, 2002; Yin *et al.*, 2001; Zhang *et al.*, 2014). A large number of data were derived from volcanic ash beds or clay beds close to the PTB, including the one in this study. The ultimate goal of this paper is to determine the age of the C_1 coal seam. In comparison with organic-poor successions, the coal beds obviously contain more information of palaeobotany, palaeoclimate and palaeoenvironment that may help better understand the PTB events. In fact, in addition the dating work of the C_1 coal seam, the palynological assemblage analysis of the C_1 coal seam had been undertaken at the same time, and the detailed description and analysis of sporopollen results will be reported in another paper.

Each tonstein layer is a record of volcanic eruption. The only 5-cm-thick tonstein implies a short eruption. He *et al.* (2007) reported that sediments of the upper Xuanwei Formation surrounding the Khangdian Oldland were derived from mafic volcanic rocks of the Emeishan large igneous province (ELIP). In view of
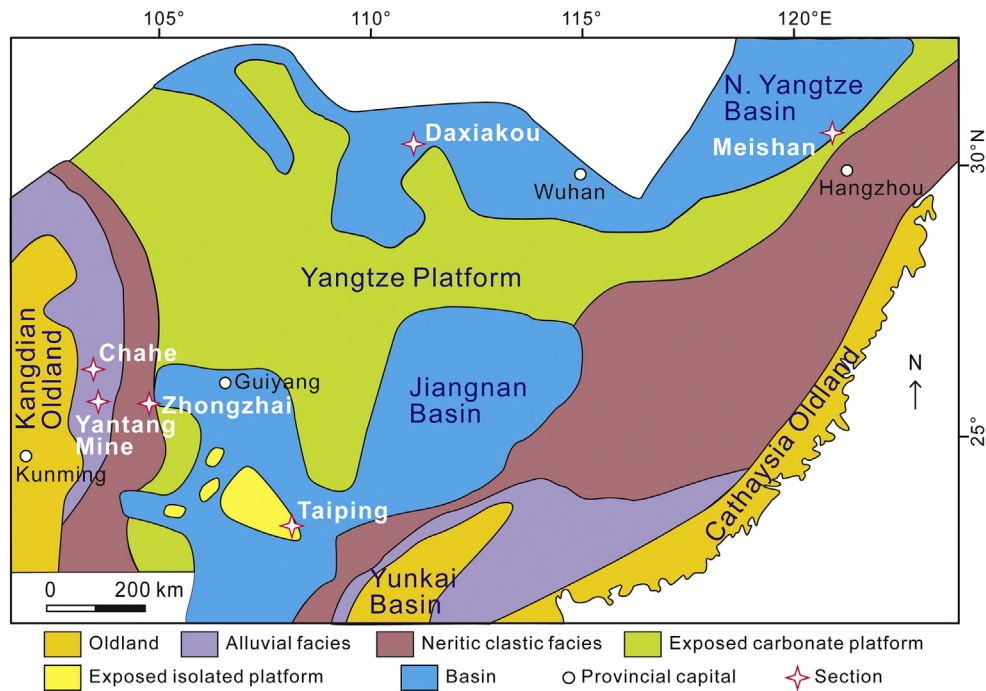
Fig. 7 Changhsingian palaeogeographic map of the South China, showing locality of the PTB sections with U—Pb dating ages (modified from Yin *et al.*, 2014).

volcanic eruptions close to the PTB, the main episode of Siberian large igneous province (SLIP) was around 252 Ma (Jerram *et al.*, 2016; Ogden and Sleep, 2012), while the terminal age of ELIP is 251.0 ± 1.0 Ma (Zhu *et al.*, 2011). It is clear that the ages of the tonsteins in the C_1 coal seam, determined in this paper, is within the range of both the ELIP and SLIP, and as a result, the origin of the tonsteins in the C_1 coal seam is hard to

determine. However, considering the distribution of large igneous provinces, the ELIP is much closer to Xuanwei County than SLIP. The closest ELIP eruption site with available research data is in Dongchuan, eastern Yunnan, some 109 km to the west-southwest (Xu *et al.*, 2001). According to the spatial and temporal distribution of ELIP, we interpret the tonsteins analyzed in this study to have formed by volcanic
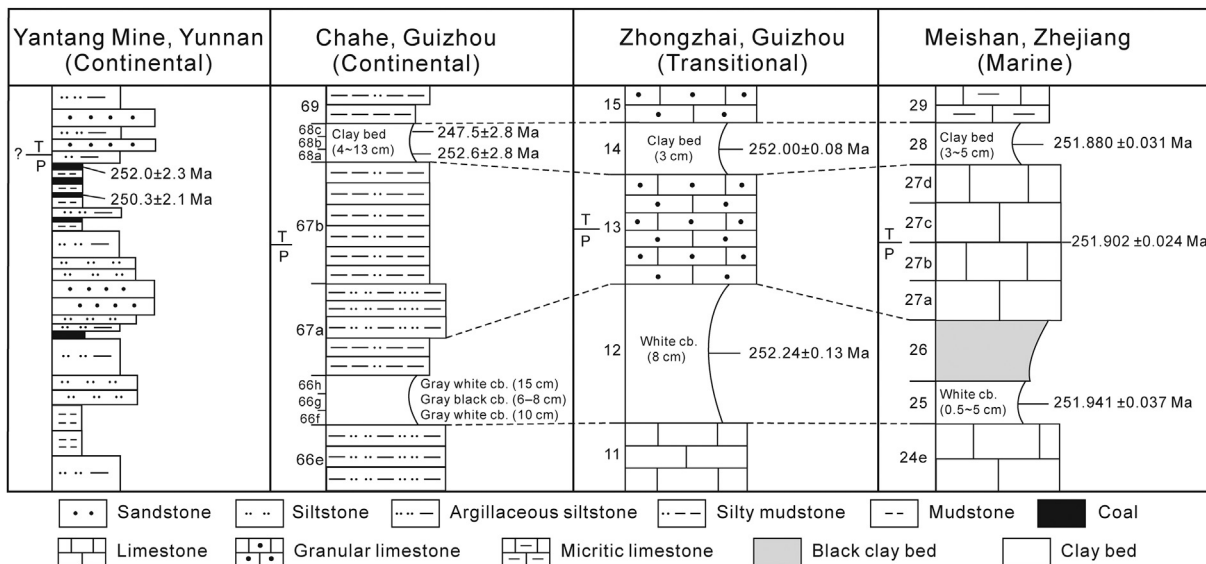

Fig. 8 Correlation of PTB sections in South China (modified after Yin *et al.*, 2007). Source of ages: Yantang Mine, this study; Chahe section, Yang *et al.* (2005) and Yin *et al.* (2007); Zhongzhai section, Shen *et al.* (2011); Meishan section, Burgess *et al.* (2014), Shen *et al.* (2011), and Yin and Song (2013). cb. = Clay bed.

eruptions of the ELIP. Furthermore, the minerals and geochemistry characteristics (Shao et al., 2015) of the C_1 coal also implied the influence of contemporaneous volcanic activities.

As the last coal deposited at the end Permian, the C_1 coal seam in Yantang Mine contains abundant information, such as carbon and sulfur isotope, minerals, poisonous and harmful trace elements, and organic macerals. These geochemical characteristics of the C_1 coal seam may provide critical information about the PTB events, which most importantly, is the largest mass extinction event in the Earth history.

6.   Conclusions

Two partings from the C_1 coal seam in the Yantang Mine, Xuanwei, eastern Yunnan, China, close to the PTB were investigated. Their mineralogical composition indicates that these partings are tonsteins derived from volcanic ash. The coal itself is enriched with silica derived probably from a volcanic source. The SHRIMP zircon U—Pb ages of these tonsteins are 252.0 ± 2.3 Ma and 250.3 ± 2.1 Ma, which are compatible to the U—Pb zircon age of main episode of PTB mass extinction (Bed 25) from the most extensively-studied Meishan section, Zhejiang Province, China. In particular, the age of upper tonstein B_1-3 dated as 252.0 ± 2.3 Ma is a little older than Bed 25 at Meishan, which means the coal-forming plant of C_1 coal seam occurred just before the end-Permian mass extinction. Spatial and temporal analyses suggest that volcanic ashes that formed the tonsteins in the C_1 coal seam were likely from the ELIP. These findings encourage further research on the biological, mineralogical and geochemical features of the coal beds and tonstein layers near the PTB in South China.

Acknowledgements

References

Black, L.P., Jagodzinski, E.A., 2003. Importance of establishing sources of uncertainty for the derivation of reliable SHRIMP ages. Australian Journal of Earth Sciences, 50(4), 503—512.

Bowring, S.A., Erwin, D.H., Jin, M.W.M.Y., Davidek, K., Wang, W., 1998. U/Pb zircon geochronology and tempo of the end-Permian mass extinction. Science, 280(5366), 1039—1045.

Burgess, S.D., Bowring, S., Shen, S.Z., 2014. High-precision timeline for Earth's most severe extinction. Proceedings of the National Academy of Sciences of the United States of America, 111(9), 3316—3321.

Compston, W., Williams, I.S., Kirschvink, J.L., Zhang, Z.C., Ma, G.G., 1992. Zircon U—Pb ages for the early Cambrian time-scale. Journal of the Geological Society, London, 149(2), 171—184.

Dai, S.F., Tian, L.W., Chou, C.L., Zhou, Y.P., Zhang, M.Q., Zhao, L., Wang, J.M., Yang, Z., Cao, H.Z., Ren, D.Y., 2008. Mineralogical and compositional characteristics of Late Permian coals from an area of high lung cancer rate in Xuan Wei, Yunnan, China: Occurrence and origin of quartz and chamosite. International Journal of Coal Geology, 76(4), 318—327.

Gao, Q.L., Zhang, N., Xia, W.C., Feng, Q.L., Chen, Z.Q., Zheng, J.P., Griffin, W.L., O'Reilly, S.Y., Pearson, N.J., Wang, G.Q., Wu, S., Zhong, W.L., Sun, X.F., 2013. Origin of volcanic ash beds across the Permian—Triassic boundary, Daxiakou, South China: Petrology and U—Pb age, trace elements and Hf-isotope composition of zircon. Chemical Geology, 360—361, 41—53.

He, B., Xu, Y.G., Huang, X.L., Luo, Z.Y., Shi, Y.R., Yang, Q.J., Yu, S.Y., 2007. Age and duration of the Emeishan flood volcanism, SW China: Geochemistry and SHRIMP zircon U—Pb dating of silicic ignimbrites, post-volcanic Xuanwei Formation and clay tuff at the Chaotian section. Earth and Planetary Science Letters, 255(3—4), 306—323.

Hoskin, P.W.O., Schaltegger, U., 2003. The composition of zircon and igneous and metamorphic petrogenesis. Reviews in Mineralogy and Geochemistry, 53(1), 27—62.

ICS (International Commission on Stratigraphy), 2017. International Chronostratigraphic Chart. http://www.stratigraphy.org/2016/04.

Jerram, D.A., Svensen, H.H., Planke, S., Polozov, A.G., Torsvik, T.H., 2016. The onset of flood volcanism in the north-western part of the Siberian Traps: Explosive volcanism versus effusive lava flows. Palaeogeography, Palaeoclimatology, Palaeoecology, 441(Part 1), 38—50.

Jiang, H.S., Lai, X.L., Luo, G.M., Aldridge, R., Zhang, K.X., Wignall, P., 2007. Restudy of conodont zonation and evolution across the P/T boundary at Meishan section, Changxing, Zhejiang, China. Global and Planetary Change, 55(1—3), 39—55.

Kozur, H.W., 2003. Integrated ammonoid, conodont and radiolarian zonation of the Triassic and some remarks to Stage/Substage subdivision and the numeric age of the Triassic stages. Albertiana, 28, 57—74.

Lehrmann, D.J., Stepchinski, L., Altiner, D., Orchard, M.J., Montgomery, P., Enos, P., Ellwood, B.B., Bowring, S.A., Ramezani, J., Wang, H.M., Wei, J.Y., Yu, M.Y., Griffiths, J.D., Minzoni, M., Schaal, E.K., Li, X.W., Meyer, K.M., Payne, J.L., 2015. An integrated biostratigraphy (conodonts and foraminifers) and chronostratigraphy (paleomagnetic reversals, magnetic susceptibility,

elemental chemistry, carbon isotopes and geochronology) for the Permian—Upper Triassic strata of Guandao section, Nanpanjiang Basin, South China. *Journal of Asian Earth Sciences*, 108, 117—135.

Li, Z.X., Xie, S.K., He, J.L., Xiong, S., Wu, T., Deng, Q., 2014. LA-ICP-MS U—Pb zircon dating of dioritic gneiss and its geochemical characteristics in the Lianggehu region, Qiangtang Basin. *Acta Geologica Sinica*, 88(1), 15—24 (in Chinese with English abstract).

Liu, J.H., Liu, D.Y., Zhang, Y.H., Yang, Z.Q., 2011. Techniques for choosing target points during SHRIMP dating of zircon U—Pb ages. *Rock and Mineral Analysis*, 30(3), 265—268 (in Chinese with English abstract).

Ludwig, K.R., 2003. *Isoplot/ex Version 3.0: a Geochronological Toolkit for Microsoft Excel*. Berkeley Geochronology Center, Special Publication, Berkeley.

Mundil, R., Ludwig, K.R., Metcalfe, I., Renne, P.R., 2004. Age and timing of the Permian mass extinctions: U/Pb dating of closed-system zircons. *Science*, 305(5691), 1760—1763.

Nicoll, R.S., Metcalfe, I., Wang, C.Y., 2002. New species of the conodont genus *Hindeodus* and the conodont biostratigraphy of the Permian—Triassic boundary interval. *Journal of Asian Earth Sciences*, 20(6), 609—631.

Ogden, D.E., Sleep, N.H., 2012. Explosive eruption of coal and basalt and the end-Permian mass extinction. *Proceedings of the National Academy of Sciences of the United States of America*, 109(1), 59—62.

Peng, Y.Q., Yin, H.F., Yang, F.Q., 2001. Advance in the study of terrestrial Permian—Triassic boundary. *Advances in Earth Sciences*, 16(6), 769—776 (in Chinese with English abstract).

Peng, Y.Q., Zhang, S.X., Yu, T.X., Yang, F.Q., Gao, Y.Q., Shi, G.R., 2005. High-resolution terrestrial Permian—Triassic eventostratigraphic boundary in western Guizhou and eastern Yunnan, southwestern China. *Palaeogeography, Palaeoclimatology, Palaeoecology*, 215(3—4), 285—295.

Retallack, G.J., Veevers, J.J., Morante, R., 1996. Global coal gap between Permian—Triassic extinction and Middle Triassic recovery of peat-forming plants. *GSA Bulletin*, 108(2), 195—207.

Shao, L.Y., Liu, H.M., Tian, B.L., Zhang, P.F., 1998. Sedimentary evolution and its controls on coal accumulation for the Late Permian in the Upper Yangtze area. *Acta Sedimentologica Sinica*, 16(2), 55—60 (in Chinese with English abstract).

Shao, L.Y., Wang, H., Yu, X.H., Lu, J., Zhang, M.Q., 2012. Paleo-fires and atmospheric oxygen levels in the latest Permian: Evidence from maceral compositions of coals in eastern Yunnan, southern China. *Acta Geologica Sinica (English Edition)*, 86(4), 949—962.

Shao, L.Y., Wang, J., Hou, H.H., Zhang, M.Q., Wang, H., Spiro, B., Large, D., Zhou, Y.P., 2015. Geochemistry of the C_1 coal of latest Permian during mass extinction in Xuanwei, Yunnan. *Acta Geologica Sinica*, 89(1), 163—179 (in Chinese with English abstract).

Shao, L.Y., Zhang, P.F., Dou, J.W., Shen, S.Z., 2000. Carbon isotope compositions of the late Permian carbonate rocks in southern China: Their variations between the wujiaping and Changxing formations. *Palaeogeography, Palaeoclimatology, Palaeoecology*, 161(1—2), 179—192.

Shen, S.Z., Crowley, J.L., Wang, Y., Bowring, S.A., Erwin, D.H., Sadler, P.M., Cao, C.Q., Rothman, D.H., Henderson, C.M., Ramezani, J., Zhang, H., Shen, Y.A., Wang, X.D., Wang, W., Mu, L., Li, W.Z., Tang, Y.G., Liu, X.L., Liu, L.J., Zeng, Y., Jiang, Y.F., Jin, Y.G., 2011. Calibrating the end-Permian mass extinction. *Science*, 334(6061), 1367—1372.

Song, B., Zhang, Y.H., Wan, Y.S., Jian, P., 2002. Mount making and procedure of the SHRIMP dating. *Geological Review*, 48(Supplment), 26—30 (in Chinese with English abstract).

Wang, H., Shao, L.Y., Hao, L.M., Zhang, P.F., Glasspool, I.J., Wheeley, J.R., Wignall, P.B., Yi, T.S., Zhang, M.Q., Hilton, J., 2011. Sedimentology and sequence stratigraphy of the Lopingian (Late Permian) coal measures in southwestern China. *International Journal of Coal Geology*, 85(1), 168—183.

Wang, Y., Jin, Y.G., 2000. Permian palaeogeographic evolution of the jiangnan basin, South China. *Palaeogeography, Palaeoclimatology, Palaeoecology*, 160(1—2), 35—44.

Wu, Y.B., Zheng, Y.F., 2004. Mineralogical study on zircon genesis and its constraints on interpreting U—Pb age. *Chinese Science Bulletin*, 49(16), 1589—1604 (in Chinese).

Xu, Y.G., Chung, S.-L., Jahn, B.-M., Wu, G.Y., 2001. Petrologic and geochemical constraints on the petrogenesis of Permian—Triassic Emeishan flood basalts in southwestern China. *Lithos*, 58(3—4), 145—168.

Yang, F.Q., Yin, H.F., Yu, J.X., Zhang, S.X., Huang, J.H., Peng, Y.Q., Huang, Q.S., Zhao, Q.M., 2005. Stratigraphical study on the terrestrial Permian—triassic boundary at Chahe section, weining County, Guizhou province, China. *Science in China Series D: Earth Sciences*, 35(6), 519—529 (in Chinese).

Yin, H.F., Jiang, H.S., Xia, W.C., Feng, Q.L., Zhang, N., Shen, J., 2014. The end-Permian regression in South China and its implication on mass extinction. *Earth-Science Reviews*, 137(Suppl. C), 19—33.

Yin, H.F., Song, H.J., 2013. Mass extinction and Pangea integration during the Paleozoic—mesozoic transition. *Science China Earth Sciences*, 56(11), 1791—1803.

Yin, H.F., Xie, S.C., Luo, G.M., Algeo, T.J., Zhang, K.X., 2012. Two episodes of environmental change at the Permian—Triassic boundary of the GSSP section Meishan. *Earth-Science Reviews*, 115(3), 163—172.

Yin, H.F., Yang, F.Q., Yu, J.X., Peng, Y.Q., Wang, S.Y., Zhang, S.X., 2007. An accurately delineated Permian—Triassic boundary in continental successions. *Science in China Series D: Earth Sciences*, 50(9), 1281—1292.

Yin, H.F., Zhang, K.X., Tong, J.N., Yang, Z.Y., Wu, S.B., 2001. The global stratotype section and point (GSSP) of the Permian—Triassic boundary. *Episodes*, 24(2), 102—114.

Zhang, Y., Zhang, K.X., Shi, G.R., He, W.H., Yuan, D.X., Yue, M.L., Yang, T.L., 2014. Restudy of conodont biostratigraphy of the Permian—triassic boundary section in Zhongzhai, southwestern Guizhou province, South China. *Journal of Asian Earth Sciences*, 80, 75—83.

Zhou, Y.P., Bohor, B.F., Ren, Y.L., 2000. Trace element geochemistry of altered volcanic ash layers (tonsteins) in Late Permian coal-bearing formations of eastern Yunnan and western Guizhou Provinces, China. *International Journal of Coal Geology*, 44(3), 305—324.

Zhou, Y.P., Ren, Y.L., 1994. Element geochemistry of volcanic ash derived tonsteins in Late Permian coal-bearing formation of eastern Yunnan and western Guizhou, China. *Acta Sedimentologica Sinica*, 12(2), 123—132 (in Chinese with English abstract).

Zhu, J., Zhang, Z.C., Hou, T., Kang, J.L., 2011. LA-ICP-MS zircon U—Pb geochronology of the tuffs on the uppermost of the Emeishan basalt succession in Panxian County, Guizhou Province: Constraints on genetic link between Emeishan large igneous province and the mass extinction. *Acta Petrologica Sinica*, 27(9), 2743—2751 (in Chinese with English abstract).